Title

Tidal end states of binary asteroid systems with a nonspherical component

Authors

Taylor, PA

Margot, JL

Tidal End States of Binary Asteroid Systems
with a Nonspherical Component

Patrick A. Taylor[a,*] and *Jean-Luc Margot*[b]
[a]*Arecibo Observatory*, [b]*UCLA*

ptaylor@naic.edu

ABSTRACT: We derive the locations of the fully synchronous end states of tidal evolution for binary asteroid systems having one spherical component and one oblate- or prolate-spheroid component. Departures from a spherical shape, at levels observed among binary asteroids, can result in the lack of a stable tidal end state for particular combinations of the system mass fraction and angular momentum, in which case the binary must collapse to contact. We illustrate our analytical results with near-Earth asteroids (8567) 1996 HW_1, (66391) 1999 KW_4, and 69230 Hermes.

1. Introduction

Recent studies have examined energy, stability, and orbital relative equilibria in the planar two-body problem for a non-rotating sphere and an arbitrary, rotating ellipsoid (Scheeres, 2007; Bellerose and Scheeres, 2008) and approximately for two arbitrary, rotating ellipsoids (Scheeres, 2009). Here, we examine the special case of a rotating sphere interacting with a rotating oblate or prolate spheroid and provide exact, tractable analytical results for the locations of the fully synchronous end states of tidal evolution. The terms fully synchronous tidal end state and orbital relative equilibrium can be used interchangeably to describe a zero-eccentricity binary system that has ceased tidally evolving because the spin rates of both components have synchronized to the mean motion of the components about the center of mass of the system.

This note is organized as follows. In Section 2, we review fully synchronous tidal end states of a binary system consisting of two spheres. Section 3 extends the discussion to a sphere interacting with an ellipsoid and explores the specific cases of oblate and prolate spheroids with applications to real asteroid systems. Comparisons to previous work in Sections 3 and 4 place this work in context and possible avenues for contact-binary formation are suggested.

2. Fully synchronous orbits with spherical components

The locations of the fully synchronous end states of tidal evolution for binary asteroids with spherical components were discussed by Taylor and Margot (2011) and are summarized here. For components of equal, uniform density ρ with radii R_1 and R_2 and mass ratio $q = M_2/M_1 = (R_2/R_1)^3$ separated by a distance a in their circular mutual orbit, the sum of the orbital and spin angular momentum J upon full synchronization, scaled by $J' = \sqrt{G(M_1 + M_2)^3 R_{\mathrm{eff}}}$, where R_{eff} is the effective radius of a sphere with the same volume as both components combined, is:

$$\frac{J}{J'} = \frac{q}{(1+q)^{13/6}} \left(\frac{a}{R_1}\right)^{1/2} + \frac{2}{5} \frac{1+q^{5/3}}{(1+q)^{7/6}} \left(\frac{a}{R_1}\right)^{-3/2} \tag{1}$$

[cf. Taylor and Margot (2011), Eq. (8)]. The term on the left, proportional to $a^{1/2}$, is the orbital angular momentum of the system revolving with mean motion n, given by Kepler's Third Law, scaled by J'. The term on the right, proportional to $a^{-3/2}$, is the spin angular momentum of the two components, both rotating with spin rate n, scaled by J'. The $1 + q^{5/3}$ term is proportional to the sum of the moments of inertia of the two bodies; removing the $q^{5/3}$ term amounts to ignoring the spin angular momentum of component 2. Depending on the mass ratio and the total angular momentum of the system, Eq. (1) may have zero, one (degenerate), or two solutions (one unstable

2

and one stable), corresponding to the number of fully synchronous orbits supported by the system. The total energy when the system has fully synchronized may be positive or negative depending on the parameters of the system. One can show that the zero-energy limit always falls within the stability limit that splits the unstable and stable solutions such that all stable, fully synchronous orbits have negative energy, *i.e.*, they are gravitationally bound.

For plotting purposes, we transform from mass ratio q to mass fraction $v = M_2/(M_1 + M_2)$ and scale the separation a by $R_1 + R_2$, the contact limit. Figure 1 shows, for a two-sphere binary system, the locations of the fully synchronous orbits using contours of angular momentum J/J'. Because the components are similar in shape, the diagram is mirror symmetric about $v = 0.5$; this will not be the case when one component is nonspherical. Unstable inner synchronous orbits, the solutions below the stability limit in Fig. 1, almost always fall within the contact limit, with the exception of the $J/J' = 0.25$ curve, similar to the angular momentum found in most large main-belt binary systems likely formed by collisions. In systems with $J/J' \sim 0.4$, similar to near-Earth binaries and small main-belt binaries likely formed via spin-up processes, the secondary is formed beyond the inner synchronous orbit and will naturally tidally evolve outward, vertically through the diagram, until reaching the outer synchronous orbit at the intersection with its corresponding angular-momentum contour. Of course, this is a simplistic view because the post-fission dynamical environment of a newly formed binary asteroid is chaotic (Jacobson and Scheeres, 2011), carrying the risk of ejection or re-impact of the secondary or the secondary itself undergoing fission. Once the system has settled, the steady, comparatively quiescent, tidal evolution to the outer synchronous orbit continues as in Fig. 1. An equal-mass binary with $v = 0.5$ must have $J/J' > 0.44$ (more exactly, 0.43956) to have a stable tidal end state.

3. Fully synchronous orbits with a nonspherical component

Let component 1 of the binary system be a uniform-density ellipsoid with principal semi-axes $a_0 \geq a_1 \geq a_2$ such that the equivalent radius of the ellipsoid is $R_1 = (a_0 a_1 a_2)^{1/3}$. For rotation about the shortest principal axis, the ratio of the moment of inertia of the ellipsoid to that of its equivalent-volume sphere with radius R_1 is the nonsphericity parameter (Descamps and Marchis, 2008):

$$\lambda = \frac{1 + \beta^2}{2 (\alpha\beta)^{2/3}}, \tag{2}$$

where $\alpha = a_2/a_0$, $\beta = a_1/a_0$, and $\alpha \leq \beta \leq 1$. The nonsphericity parameter is always larger than unity because any departure from a spherical shape requires displacing mass farther from the spin axis and increases the moment of inertia of the body. Component 2 is assumed to remain spherical. To retain orbital relative equilibrium, the sphere must orbit above one of the principal axes of the ellipsoid and the system must rotate about another principal axis of the ellipsoid at a specific rate (Scheeres, 2006) given by:

$$n^2 = \frac{3}{2} G (M_1 + M_2) \int_{r^2 - a_i^2}^{\infty} \frac{\mathrm{d}u}{(a_i^2 + u) \Delta(u)} \tag{3}$$

[cf. Scheeres (2007), Eq. (18)], where $\Delta(u) = \sqrt{(a_0^2 + u)(a_1^2 + u)(a_2^2 + u)}$, a_i is the principal semi-axis that the sphere orbits above, and r is the orbital separation of the bodies (r is the semimajor axis a for the circular orbits considered here). Defining $\bar{a} = a/a_0$ and $u' = u/a_0^2$, the
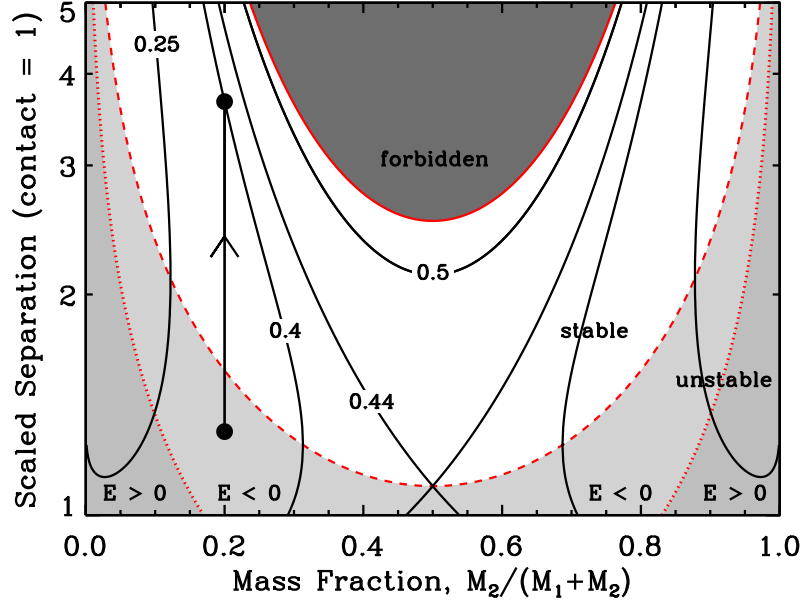
Fig. 1.— Component separation a, scaled to the contact limit, for the fully synchronous orbits of a two-sphere binary system with mass fraction v and angular momentum J/J'. The black curves indicate the inner (when not within contact limit) and outer synchronous orbits for $J/J' = 0.25, 0.4, 0.44$ and 0.5. The red dotted curve is the zero-energy limit; tidal end states above this limit have negative energy ($E < 0$) and must remain bound. The red dashed curve is the stability limit that splits the unstable inner orbits in the gray regions from the stable outer orbits in the white region. The darkest region above the solid red line represents the angular-momentum limit for $J/J' = 0.5$ and is inaccessible to systems with $J/J' \leq 0.5$. See Section 3.1 and Taylor and Margot (2011) for details on these limits. A binary system tidally evolves upward along a vertical line at mass fraction v, away from the gray regions and into the white region, where it reaches the stable outer synchronous orbit at the intersection with its corresponding J/J' contour. A $v = 0.2$ ($q = 0.25$) binary system with $J/J' = 0.4$ is shown evolving from a state initially near contact.

4

mean motion becomes:

$$n^2 = \frac{G\left(M_1 + M_2\right)}{a^3} f\left(\alpha, \beta, \bar{a}, a_i\right), \tag{4}$$

introducing f as the dimensionless integral:

$$f\left(\alpha, \beta, \bar{a}, a_i\right) = \frac{3}{2}\bar{a}^3 \int_{\bar{a}^2 - \left(\frac{a_i}{a_0}\right)^2}^{\infty} \frac{\mathrm{d}u'}{\left(\left(\frac{a_i}{a_0}\right)^2 + u'\right)\sqrt{\left(1 + u'\right)\left(\alpha^2 + u'\right)\left(\beta^2 + u'\right)}}. \tag{5}$$

For two spheres, Eq. (4) simplifies to Kepler's Third Law as the integral f goes to unity. To apply this condition to an ensemble of systems while accounting for the spins of both components and the orbital mean motion, we use a dimensionless form of the angular momentum that is applicable to binary systems with any absolute size, mass, and separation. Starting from Eq. (1), when component 1 is nonspherical, the effective radius R_1 is by definition $(\alpha\beta)^{1/3} a_0$, the contribution of the (scaled) moments of inertia of the two components to the spin angular momentum increases from $1 + q^{5/3}$ to $\lambda + q^{5/3}$, and the mean motion n includes the additional factor of $f\left(\alpha, \beta, \bar{a}, a_i\right)^{1/2}$ compared to the two-sphere case. Upon simplification, the total angular momentum J/J' of a sphere and ellipsoid in a fully synchronous orbit satisfies:

$$\frac{J}{J'} = (\alpha\beta)^{-1/6} \left[\frac{q}{(1+q)^{13/6}} \bar{a}^{1/2} + \frac{2}{5}\frac{1}{(1+q)^{7/6}} \left(\frac{1+\beta^2}{2} + (\alpha\beta)^{2/3} q^{5/3} \right) \bar{a}^{-3/2} \right] \left[f\left(\alpha, \beta, \bar{a}, a_i\right) \right]^{1/2}, \tag{6}$$

recalling that $\bar{a} = a/a_0$. In the limit that the nonspherical component approaches a sphere, α, β, and the integral f go to unity and $\bar{a}$ is equivalent to a/R_1, which recovers the two-sphere case of Eq. (1) explored by Taylor and Margot (2011) and shown in Fig. 1.

3.1. Angular-momentum, stability, and zero-energy limits

Three dynamical limits: the angular-momentum limit, the stability limit, and the zero-energy limit, break up the parameter space of mass fraction and separation, and all three depend on the shape of the nonspherical component of the binary system. The angular-momentum limit follows from Eq. (6) by setting the spin angular momentum (the term proportional to $\bar{a}^{-3/2}$) to zero and rearranging such that the maximum separation of the components $\bar{a}_{\max} = a_{\max}/a_0$ for a given angular momentum J/J' is the numerical solution to:

$$\bar{a}_{\max} f\left(\alpha, \beta, \bar{a}_{\max}, a_i\right) = (\alpha\beta)^{1/3} \frac{(1+q)^{13/3}}{q^2} \left(J/J'\right)^2. \tag{7}$$

In the limit that the nonspherical shape approaches a sphere, α, β, and f go to unity, reproducing the two-sphere result [cf. Taylor and Margot (2011), Eq. (5)]. The stability limit $\bar{a}_{\mathrm{stab}}$, which splits the solutions to Eq. (6) into unstable inner and stable outer orbits, is given by the root of:

$$\frac{\mathrm{d}}{\mathrm{d}\bar{a}} \left[\frac{J}{J'}\left(\alpha, \beta, \bar{a}, a_i\right) \right] = 0. \tag{8}$$

Due to the complicated dependence of the integral in Eq. (6) on separation, the stability limit is not algebraic as in the two-sphere case [cf. Taylor and Margot (2011), Eq. (11)] and is left to a numerical solution.

5

The total energy of a binary system is given by the sum of the rotational, orbital, and gravitational potential energies. When the components are fully synchronized to the orbital mean motion n:

$$E = \frac{1}{2} \frac{M_1 M_2}{M_1 + M_2} a^2 n^2 + \frac{1}{2} I_1 n^2 + \frac{1}{2} I_2 n^2 + V, \tag{9}$$

where the rotational energy is in terms of the polar moments of inertia I of the components, $(2/5) M R^2$ for a sphere and a factor of λ greater for an ellipsoid. The gravitational potential energy V (e.g., Scheeres, 1994, and references therein) can be written as:

$$V = -\frac{G M_1 M_2}{a} \left[\frac{3}{4} \bar{a} \int_{\bar{a}^2 - \left(\frac{a_i}{a_0}\right)^2}^{\infty} \left(1 - \frac{\bar{a}^2}{\left(\frac{a_i}{a_0}\right)^2 + u'} \right) \frac{\mathrm{d}u'}{\sqrt{(1 + u')(\alpha^2 + u')(\beta^2 + u')}} \right] \tag{10}$$

when the sphere orbits above semi-axis a_i of the ellipsoid. Note the familiar result for the gravitational potential energy between two point masses, which is reproduced when the term in brackets goes to unity for two spheres. One can split the integral for V into two terms and define another dimensionless integral:

$$g(\alpha, \beta, \bar{a}, a_i) = \frac{3}{2} \bar{a} \int_{\bar{a}^2 - \left(\frac{a_i}{a_0}\right)^2}^{\infty} \frac{\mathrm{d}u'}{\sqrt{(1 + u')(\alpha^2 + u')(\beta^2 + u')}} \tag{11}$$

similar to f. Then, for the instance when the total energy E is zero, after applying Eq. (4), the critical separation $\bar{a}_{\mathrm{E}}$ satisfies:

$$\bar{a}_{\mathrm{E}} \left[\frac{g(\alpha, \beta, \bar{a}_{\mathrm{E}}, a_i)}{f(\alpha, \beta, \bar{a}_{\mathrm{E}}, a_i)} - 2 \right]^{1/2} = \left[\frac{2}{5} \frac{1 + q}{q} \left(\frac{1 + \beta^2}{2} + (\alpha\beta)^{2/3} q^{5/3} \right) \right]^{1/2}, \tag{12}$$

which recovers the two-sphere, zero-energy limit [cf. Taylor and Margot (2011), Eq. (15)] as α and β go to unity and $g/f \to 3$.

3.2. Comparison to previous work

Scheeres (2007) and Bellerose and Scheeres (2008) analyze a planar two-body problem consisting of a triaxial ellipsoid and a sphere in mutual orbit. Concentrating on Bellerose and Scheeres (2008), our analysis follows similarly, but with two key differences. First, we normalize the total angular momentum as J/J', while they normalize their angular momentum K [cf. Bellerose and Scheeres (2008), Eq. (18)] such that:

$$J/J' = (\alpha\beta)^{-1/6} v (1 - v)^{7/6} K. \tag{13}$$

The second important difference is that we account for the spin angular momentum of the sphere, the $q^{5/3}$ term in Eqs. (1) and (6), which makes a non-negligible contribution in equal-mass binaries and when the sphere is the primary component. As a result, Eq. (13) must be supplemented by the spin angular momentum of the sphere scaled by J'. Scheeres (2007) also ignores the spin angular momentum of the sphere in orbit because, under ideal conditions, a perfect sphere in orbit cannot be tidally torqued or transfer angular momentum, but we consider the sphere to have a slight tidal or permanent deformation to allow for spin-orbit coupling even though it is treated mathematically as a sphere. Combining these two points prevents a one-to-one mapping between

the results of this work for a value of J/J' and those of Bellerose and Scheeres (2008) for a value of K, though the curves that trace out our fully synchronous orbits and their orbital relative equilibria, as well as the stability and zero-energy limits, have the same inherent meanings. The difference between these approaches is evident when comparing the shapes of the curves in our Fig. 1 to those in Figs. 7 and 8 of Scheeres (2007) and Fig. 6 of Bellerose and Scheeres (2008).

Scheeres (2009) considers binary systems of two triaxial ellipsoids and expands the gravitational potential between the components to second order in the moments of inertia. In this work, we use the exact form of the gravitational potential in Eq. (10), which leads to the equilibrium condition in Eq. (3). In the limiting cases of spheres interacting with oblate and prolate spheroids, we can test the accuracy of the Scheeres (2009) method. The key difference between our end states and the equilibria of Scheeres (2009) is that we use a single value of angular momentum for all mass fractions, while, for each mass fraction, Scheeres (2009) uses the specific value of angular momentum that allows the components to fission from contact. In other words, Scheeres (2009) uses the angular-momentum value that has an unstable inner synchronous orbit at the contact limit for that specific mass fraction, which prevents a direct one-to-one mapping of our results to theirs.

3.3. Oblate component, $a_2 < a_1 = a_0$

In near-Earth binary asteroid systems, the rapid rotation of the primary component tends to produce an oblate shape with loose regolith built up in a circular equatorial belt, *e.g.*, the primary component of (66391) 1999 KW_4 (Ostro et al., 2006). For an oblate spheroid with identical equatorial principal axes rotating about the shortest principal axis, the semi-axes $a_2 < a_1 = a_0$ ($\alpha < \beta = 1$) and $\lambda = \alpha^{-2/3}$. For the sphere along a_0 or equivalently anywhere in the equator plane of the oblate component, the dimensionless integral f from Eq. (5) simplifies to:

$$f\left(\alpha, 1, \bar{a}, a_0\right) = \frac{3}{2}\,\bar{a}^3 \int_{\bar{a}^2-1}^{\infty} \frac{\mathrm{d}u'}{\left(1+u'\right)^2 \left(\alpha^2 + u'\right)^{1/2}}. \tag{14}$$

Evaluating Eq. (14) and substituting into Eq. (4), the necessary spin rate for orbital relative equilibrium, in terms of the uniform density ρ of the components, is:

$$n^2 = 2\pi\,G\rho\,(1+q)\,\frac{\alpha}{1-\alpha^2}\left[\frac{1}{\sqrt{1-\alpha^2}}\,\tan^{-1}\left(\sqrt{\frac{1-\alpha^2}{\bar{a}^2+\alpha^2-1}}\right) - \frac{1}{\bar{a}^2}\sqrt{\bar{a}^2+\alpha^2-1}\right], \tag{15}$$

recalling that $\bar{a} = a/a_0$ and $q = M_{\text{sphere}}/M_{\text{oblate}}$. The fully synchronous orbits then satisfy the angular-momentum equation from Eq. (6):

$$J/J' = \left[\frac{q}{(1+q)^{13/6}}\,\bar{a}^2 + \frac{2}{5}\frac{1}{(1+q)^{7/6}}\left(1+\alpha^{2/3}q^{5/3}\right)\right] \tag{16}$$

$$\times \left[\frac{3/2}{\alpha^{1/3}\left(1-\alpha^2\right)}\right]^{1/2}\left[\frac{1}{\sqrt{1-\alpha^2}}\,\tan^{-1}\left(\sqrt{\frac{1-\alpha^2}{\bar{a}^2+\alpha^2-1}}\right) - \frac{1}{\bar{a}^2}\sqrt{\bar{a}^2+\alpha^2-1}\right]^{1/2}.$$

The above expression describes the synchronous orbits as contours of constant J/J' for a sphere/oblate-spheroid system in the same way as Eq. (1) does for a two-sphere system. Applying the transformations $q = v/\left(1-v\right)$ and $\bar{a} = \left(1+\alpha^{1/3}q^{1/3}\right)\left[a/(a_0+R_2)\right]$ to arrive at mass fraction and separation scaled to the contact limit, the angular-momentum contours are shown in Fig. 2.

The curves in Fig. 2 are nearly symmetric about $v = 0.5$ (equal masses) with the effect of α subdued for large mass fractions where the smaller secondary is oblate rather than the larger primary component. At small mass fractions, such as that of 1999 KW$_4$, a typical near-Earth binary with $\alpha = 0.85$, the effect of primary oblateness on the curves in Fig. 2 is barely perceptible. At nearly equal masses, it is clearer that oblateness, for a given mass fraction and angular momentum, causes the inner synchronous orbit to push outward and the outer synchronous orbit to push inward by several percent, while the size of the largest supportable companion decreases (the lack of solutions near $v = 0.5$). For instance, while an angular-momentum budget of $J/J' = 0.44$ can support any two-sphere binary system, having a component with oblateness of $\alpha = 0.8$ would result in collapse to a contact binary for $v = 0.4 - 0.6$ as a stable, fully synchronous orbit no longer exists to support such a system. A system having an oblate component with $\alpha = 0.8$, such as 69230 Hermes (Margot et al., 2006), requires an increase in total angular momentum of at least 3.2% to account for the larger moment of inertia of the nonspherical component and support a spherical companion of any mass fraction. Hermes though, with an adequate angular-momentum budget of $J/J' \sim 0.5$, is not in danger of collapsing to a contact binary and has reached a stable tidal end state with a separation of roughly twice the contact limit.

3.4. Prolate component, $a_2 = a_1 < a_0$

For a prolate spheroid with two equivalent shorter principal semi-axes, one of which is aligned with the spin axis, $a_2 = a_1 < a_0$ ($\alpha = \beta < 1$) and $\lambda = \left(1 + \beta^2\right) / \left(2\beta^{4/3}\right)$. Here, we only consider the sphere orbiting above the long axis. Although the intermediate-axis case follows similarly mathematically, Scheeres (2006) has shown the intermediate-axis case is never energetically stable. When the spherical component orbits above the longest principal semi-axis a_0, the dimensionless integral f from Eq. (5) for a sphere/prolate-spheroid binary simplifies to:

$$f\left(\beta, \beta, \bar{a}, a_0\right) \;=\; \frac{3}{2}\,\bar{a}^3 \int_{\bar{a}^2-1}^{\infty} \frac{\mathrm{d}u'}{\left(1+u'\right)^{3/2}\left(\beta^2 + u'\right)}. \tag{17}$$

Evaluating Eq. (17) and substituting into Eq. (4), the necessary spin rate for orbital relative equilibrium, in terms of the uniform density ρ of the components, is:

$$n^2 \;=\; 4\pi\, G\rho\,(1+q)\,\frac{\beta^2}{1-\beta^2}\left[\frac{1}{\sqrt{1-\beta^2}}\,\tanh^{-1}\left(\frac{\sqrt{1-\beta^2}}{\bar{a}}\right) - \frac{1}{\bar{a}}\right], \tag{18}$$

recalling that $\bar{a} = a/a_0$ and $q = M_{\text{sphere}}/M_{\text{prolate}}$. The fully synchronous orbits then satisfy the angular-momentum equation from Eq. (6):

$$J/J' \;=\; \left[\frac{q}{(1+q)^{13/6}}\,\bar{a}^2 + \frac{2}{5}\,\frac{1}{(1+q)^{7/6}}\left(\frac{1+\beta^2}{2} + \beta^{4/3} q^{5/3}\right)\right] \tag{19}$$

$$\times \left[\frac{3}{\beta^{2/3}\left(1-\beta^2\right)}\right]^{1/2}\left[\frac{1}{\sqrt{1-\beta^2}}\,\tanh^{-1}\left(\frac{\sqrt{1-\beta^2}}{\bar{a}}\right) - \frac{1}{\bar{a}}\right]^{1/2}.$$

The above expression describes the synchronous orbits as contours of constant J/J' for a sphere/prolate-spheroid system in the same way as Eq. (1) does for a two-sphere system. Applying
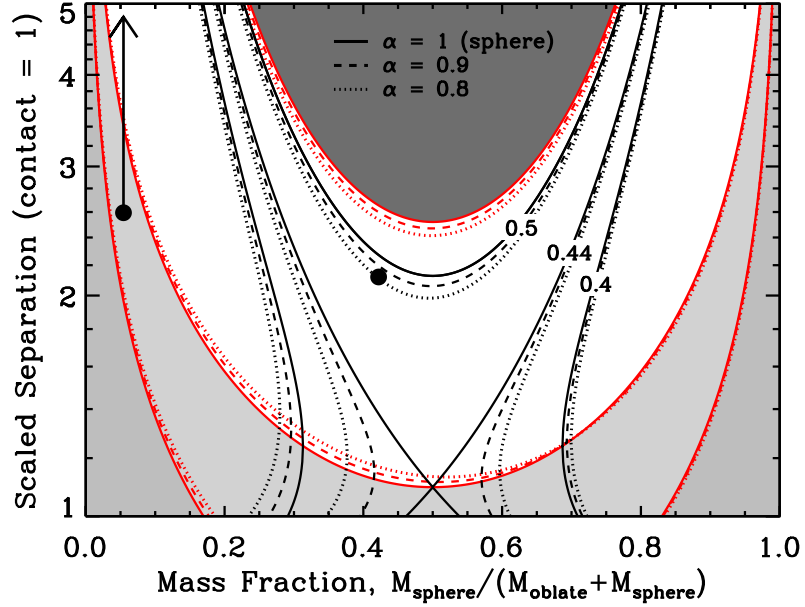
Fig. 2.— Component separation a, scaled to the contact limit, for the fully synchronous orbits of a sphere/oblate-spheroid binary system with oblateness $\alpha = 1$, 0.9, and 0.8, mass fraction v, and angular momentum $J/J' = 0.4$, 0.44, and 0.5. Solid lines correspond to the $\alpha = 1$ (two-sphere) case, dashed lines correspond to $\alpha = 0.9$, and dotted lines correspond to $\alpha = 0.8$. Red curves represent the angular-momentum, stability, and zero-energy limits as in Fig. 1. Further annotations are suppressed for clarity. The gray regions are shaded with respect to the $\alpha = 1$ case, but could be shaded for any value of α. The darkest region is inaccessible to systems with $J/J' \leq 0.5$. The current state of binary near-Earth asteroid (66391) 1999 KW_4, with oblateness $\alpha = 0.85$, is the circle at left. It will continue to tidally evolve vertically through the diagram until intersecting with the $J/J' = 0.4$ curve. At center, nearly equal-mass binary 69230 Hermes, with oblateness $\alpha = 0.8$, has reached a stable, fully synchronous state with $J/J' \sim 0.5$.

9

the transformations $q = v/(1 - v)$ and $\bar{a} = \left(1 + \beta^{2/3} q^{1/3}\right) \left[a/(a_0 + R_2)\right]$ to arrive at mass fraction and separation scaled to the contact limit, the angular-momentum contours are shown in Fig. 3.

The asymmetry across $v = 0.5$ (equal masses) is clearer in the prolate case primarily due to the wider range of β values used based on observed nonspherical asteroid shapes. Similar to the oblate case, the effect of β is more subdued for large mass fractions, where the secondary is prolate rather than the larger primary component, and most important for nearly equal-mass components. Departure from a spherical shape causes the inner synchronous orbit to push outward and the outer synchronous orbit to push inward by as much as tens of percent depending on the mass fraction and degree of prolateness of the nonspherical component, while the size of the largest supportable companion decreases (the lack of solutions near $v = 0.5$). An angular-momentum budget of $J/J' = 0.44$ can support any two-sphere binary system, but a component with prolateness $\beta = 0.75$ would result in collapse to a contact binary for $v = 0.35 - 0.6$ and roughly $v = 0.25 - 0.7$ for $\beta = 0.5$. To support a spherical companion of any mass fraction, systems with $\beta = 0.75$ and 0.5 require substantial increases in total angular momentum of at least 5.6% and 16%, respectively. As an example, we approximate contact binary (8567) 1996 HW$_1$ as a $\beta = 0.6$ prolate spheroid with a $v = 0.33$ sphere at the end of its long axis (Magri et al., 2011). Using Eq. (19), to remain in contact, J/J' must be less than 0.475, which by Eq. (18) corresponds to a density ρ greater than ~ 0.85 g cm^{-3} given its present rotation rate. The density constraint for $J/J' = 0.475$ is 15% less when using the true shape of 1996 HW$_1$ and would be more stringent for a faster rotation period.

4. Discussion

We have presented analytical formulae for contours of constant angular momentum for ensembles of binary systems consisting of an oblate/prolate component and a spherical component that, in turn, determine the fully synchronous tidal end states for specific binary systems according to their mass fractions. In retaining the spin angular momentum of the sphere, we extend the results of Bellerose and Scheeres (2008). In general, the presence of a nonspherical component breaks the symmetry about $v = 0.5$ of a two-sphere system and, for comparable angular momenta, shifts inner synchronous orbits outward and outer synchronous orbits inward and reduces the size of the largest supportable companion. At disparate mass ratios though, like those of typical near-Earth binaries, the effect of a nonspherical component on the locations of the fully synchronous tidal end states is minimal, especially given the extreme timescales required to reach them (Taylor and Margot, 2011). The strongest effect is in the nearly equal-mass regime ($v \sim 0.5$), where tidal timescales are much less than the dynamical lifetimes of asteroids. To support the same mass fraction as a two-sphere binary, the system requires a larger injection of angular momentum during binary formation to overcome the increased moment of inertia of the nonspherical primary. Once a nearly equal-mass binary is formed, and survives against re-impact while tidally evolving through the dynamically unstable region within the stability limit (Scheeres, 2009; Jacobson and Scheeres, 2011), two avenues allow collapse to a contact binary: loss of enough angular momentum, e.g., through YORP and/or BYORP thermal torques, that a stable tidal end state no longer exists for the system, or one unrelaxed component deforms to a more oblate or prolate shape that cannot support the binary with the existing angular-momentum budget. These avenues are in addition to other proposed contact-binary formation mechanisms such as a secondary-fission event resulting in the gentle impact of a smaller component onto the primary component (Jacobson and Scheeres, 2011) or the gravitational reaccumulation of coherent blocks
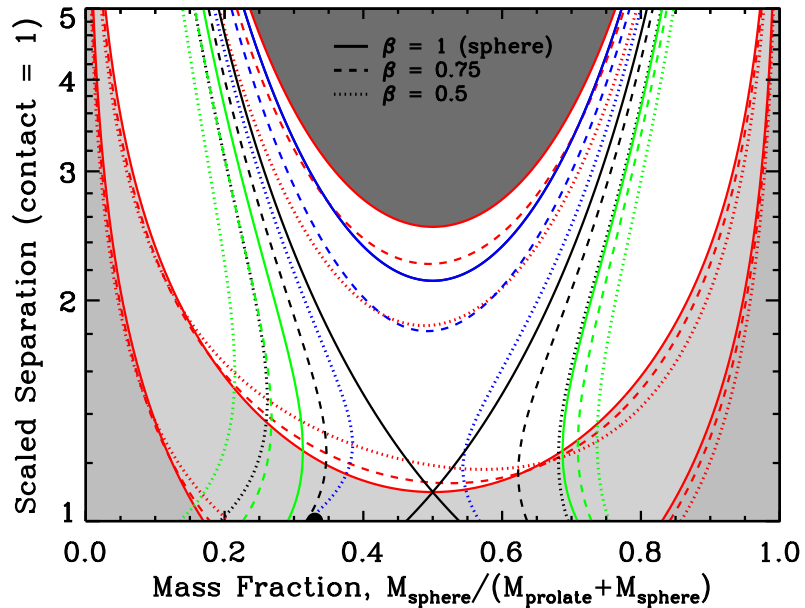
Fig. 3. Component separation a, scaled to the contact limit, for the fully synchronous orbits of a sphere/prolate-spheroid binary system with prolateness $\beta = 1$, 0.75, and 0.5, mass fraction v, and angular momentum $J/J' = 0.4$, 0.44, and 0.5, colored green, black, and blue, respectively. The sphere orbits above the long axis of the prolate spheroid. Solid lines correspond to the $\beta = 1$ (two-sphere) case, dashed lines correspond to $\beta = 0.75$, and dotted lines correspond to $\beta = 0.5$. Red curves represent the angular-momentum, stability, and zero-energy limits as in Fig. 1. Further annotations are suppressed for clarity. The gray regions are shaded with respect to the $\beta = 1$ case, but could be shaded for any value of β. The darkest region is inaccessible to systems with $J/J' \leq 0.5$. The circle on the horizontal axis at $v = 0.33$ is contact binary (8567) 1996 HW_1 with $\beta = 0.6$.

11

of debris after the catastrophic collisional disruption of a parent body (Michel and Richardson, 2013). Repeated fission and impact of the components by any of these scenarios causes a so-called contact-binary cycle (Scheeres, 2007).

The effect of a nonspherical component can shift the locations of the zero-energy and stability limits for specific binary systems by up to a few tens of percent in scaled separation compared to the two-sphere case. Despite this, the zero-energy limit crosses the contact limit near $v = 0.15 - 0.2$ and $v = 0.80 - 0.85$, similar to the ranges found by Scheeres (2009), indicating that, upon fissioning from the parent body, small secondaries are at risk of becoming gravitationally unbound from the system. The resulting asteroid pair could then have a mass ratio of less than one to four, compared to one to five in the two-sphere case, which is consistent with observation (Pravec et al., 2010). Scheeres (2009) considers extending to higher-order expansions of the gravitational potential in the future. We find that the approximate zero-energy and stability limits presented by Scheeres (2009) in the oblate case are accurate to better than 1% for $\alpha > 0.5$ compared to our solution that uses the exact gravitational potential. In the prolate case, the differences can grow to $1 - 2\%$ for $\beta = 0.75$ and $5 - 10\%$ for $\beta = 0.5$, suggesting that the Scheeres (2009) approximation is reliable for ellipsoids except in the most extreme cases of nonspherical shapes.

Acknowledgments

References

Bellerose, J., Scheeres, D. J., 2008. Energy and stability in the full two-body problem. Cel. Mech. Dyn. Astron. 100, 63–91.

Descamps, P., Marchis, F., 2008. Angular momentum of binary asteroids: Implications for their possible origin. Icarus 193, 74–84.

Jacobson, S. A., Scheeres, D. J., 2011. Dynamics of rotationally fissioned asteroids: Source of observed small asteroid systems. Icarus 214, 161–178.

Magri, C., and 25 colleagues, 2011. Radar and photometric observations and shape modeling of contact binary near-Earth asteroid (8567) 1996 HW1. Icarus 214, 210–227.

Margot, J. L., and 12 colleagues, 2006. Hermes as an exceptional case among binary near-Earth asteroids. IAU Gen. Assem. 236, (Abstract #S236–35).

Michel, P., Richardson, D. C., 2013. Collision and gravitational reaccumulation: Possible formation mechanism of the asteroid Itokawa. Astron. & Astrophys. 554, L1, 1–4.

Ostro, S. J., and 15 colleagues, 2006. Radar imaging of binary near-Earth asteroid (66391) 1999 KW4. Science 314, 1276–1280.

Pravec, P., and 25 colleagues, 2010. Formation of asteroid pairs by rotational fission. Nature 466, 1085–1088.

Scheeres, D. J., 1994. Dynamics about uniformly rotating triaxial ellipsoids: Applications to asteroids. Icarus 110, 225–238.

Scheeres, D. J., 2006. Relative equilibria for general gravity fields in the sphere-restricted full 2-body problem. Celest. Mech. Dyn. Astron. 94, 317–349.

Scheeres, D. J., 2007. Rotational fission of contact binary asteroids. Icarus 189, 370–385.

Scheeres, D. J., 2009. Stability of the planar full 2-body problem. Cel. Mech. Dyn. Astron. 104, 103–128.

Taylor, P. A., Margot, J. L., 2011. Binary asteroid systems: Tidal end states and estimates of material properties. Icarus 212, 661–676.